

1 *Supporting Information for*

2

3 **Tracer-based Characterization of Source Variations of PM<sub>2.5</sub> and Organic  
4 Carbon in Shanghai Influenced by the COVID-19 Lockdown**

5

6 Shuhui Zhu<sup>1,2</sup>, Qiongqiong Wang<sup>3</sup>, Liping Qiao<sup>1</sup>, Min Zhou<sup>1</sup>, Shan Wang<sup>2</sup>, Shengrong Lou<sup>1</sup>, Dandan  
7 Huang<sup>1</sup>, Qian Wang<sup>1</sup>, Shengao Jing<sup>1</sup>, Hongli Wang<sup>1</sup>, Changhong Chen<sup>1</sup>, Cheng Huang<sup>1,\*</sup>, Jian Zhen  
8 Yu<sup>2,3,\*</sup>

9

10

11 <sup>1</sup>State Environmental Protection Key Laboratory of the Cause and Prevention of Urban Air Pollution  
12 Complex, Shanghai Academy of Environmental Sciences, Shanghai, China

13 <sup>2</sup>Division of Environment and Sustainability, Hong Kong University of Science and Technology, Hong  
14 Kong, China

15 <sup>3</sup>Department of Chemistry, Hong Kong University of Science and Technology, Hong Kong, China

16

17 Corresponding author: Jian Zhen Yu ([jian.yu@ust.hk](mailto:jian.yu@ust.hk)) and Cheng Huang ([huangc@saes.sh.cn](mailto:huangc@saes.sh.cn))

18

19

20

21 **Contents of this file:**

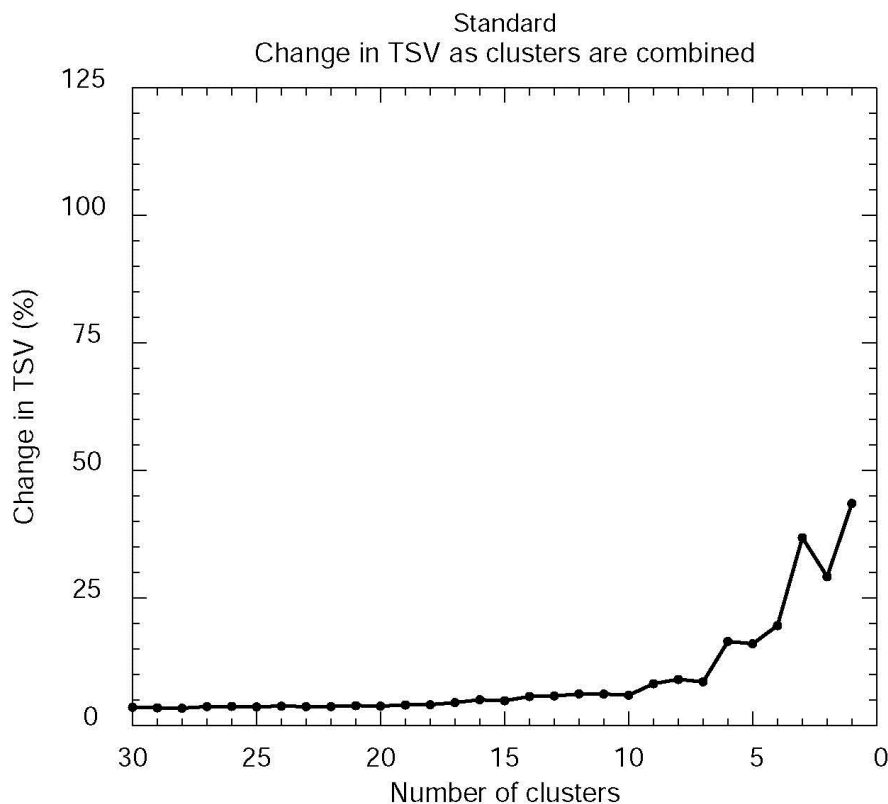
22 Text S1 to S2

23 Figures S1 to S8

24 Table S1 to S5

25 References

26



27

28 **Figure S1.** Change of total spatial variance (TSV) as a function of number of clusters at 100 m arrival  
29 height obtained from the HYSPLIT model.

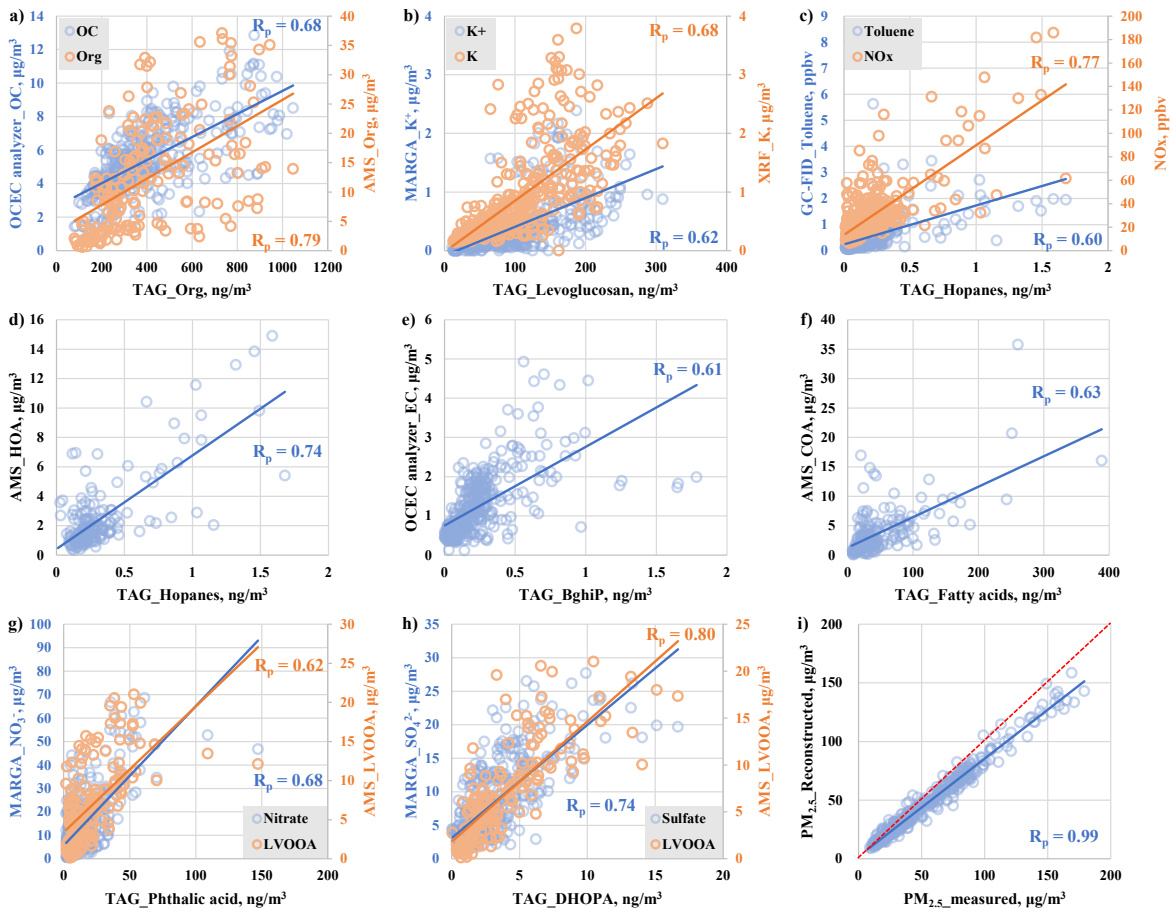
30

---

31 **Text S1. Data checking for TAG-measured organic compounds**

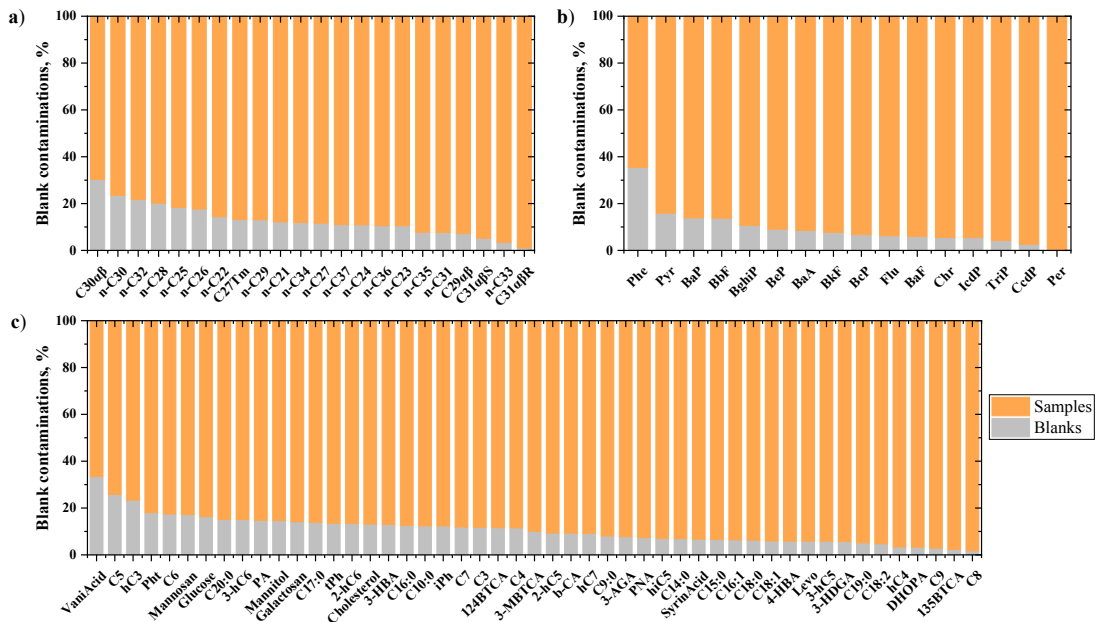
32       Taking advantage of available measurements made by multiple instruments, we carried  
33 out several internal data consistency tests between related chemical parameters measured by  
34 different instruments. Pairs of parameters are selected based on their known underlying physical  
35 relationships. Specifically, the list includes (a) the sum of 87 organic molecules measured by  
36 TAG (TAG\_Org) versus OC measured by OCEC analyzer and bulk organics in PM<sub>1</sub> measured  
37 by AMS; (b) levoglucosan measured by TAG versus K<sup>+</sup> measured by MARGA and total K  
38 measured by XRF; (c) the sum of 5 hopanes measured by TAG versus toluene measured by  
39 GC-FID and NO<sub>x</sub> measured by the NOx monitor; (d) the sum of 5 hopanes measured by TAG  
40 versus hydrocarbon-like OA (HOA) resolved by PMF analysis of mass spectra data from AMS;  
41 (e) BghiP measured by TAG versus EC obtained from OCEC analyzer; (f) the sum of 13 fatty  
42 acids measured by TAG versus cooking OA (COA) from AMS data; (g) phthalic acid measured  
43 by TAG versus nitrate measured by MARGA and low-volatility OA (LVOOA) from AMS data;  
44 (h) DHOPA (mono-aromatic compounds-derived SOA tracer) measured by TAG versus sulfate  
45 measured by MARGA and LVOOA by AMS; and (i) reconstructed versus measured PM<sub>2.5</sub>  
46 mass. Scatter correlation plots of the above pairs of parameters are illustrated in Figure S2. In  
47 general, moderate to strong correlations were observed, indicating the hourly dataset collected  
48 from different instruments are consistent with each other.

49       As part of quality control/quality assurance, blank samples were collected once every five  
50 days and a total of 7 blank samples were collected by the TAG system. The presence of the 87  
51 target organic compounds in the blank samples were either not detected or lower than 25% of  
52 the average concentration level detected in the samples for the majority of target analytes, as  
53 shown in Figure S3. Thus, the TAG-measured concentrations were not blank-corrected.



54

55 **Figure S2.** Scatter plots of select pairs of measured parameters with known underlying physical  
56 relationships. They serve as internal data consistency check.



60 **Table S1.** Statistics of hourly concentrations of 87 organic molecules measured by TAG  
 61 system, among which Abbr represents abbreviations for compound names used in this study,  
 62 organic molecules shadowed in grey refer to molecules included in PMF model.

Group	Compounds	Abbreviations	Avg ng/m <sup>3</sup>	Range ng/m <sup>3</sup>	PMF group
C <sub>3-5</sub> DCAs & hDCAs	Malonic acid	C3	11.9	0.76-70.9	LMW-DCAs
	Succinic acid	C4	21.0	1.67-167	
	Glutaric acid	C5	2.74	0.07-29.8	
	Malic_acid	hC4	15.4	BD-97.5	LMW-hDCAs
	Citramalic_acid	hiC5	4.42	0.27-23.4	
	Glyceric_acid	hC3	17.7	1.15-95.2	
	2-hydroxyglutaric acid	2-hC5	0.80	0.01-13.8	
	3-hydroxyglutaric acid	3-hC5	4.07	0.12-43.5	
C <sub>6-9</sub> DCAs & hDCAs	Adipic acid	C6	3.15	0.18-57.8	
	Pimelic acid	C7	1.22	0.05-5.99	
	Suberic acid	C8	4.25	0.06-32.0	
	Azelaic_acid	C9	4.20	0.35-26.4	
	2-hydroxyadipic acid	2-hC6	1.76	0.06-33.5	
	3-Hydroxyadipic acid	3-hC6	2.72	0.16-74.1	
	Hydroxypimelic acid	hC7	1.85	0.03-14.6	
SOA tracers	Pinic acid	PA	2.92	0.13-21.4	aPinT
	Pinonic acid	PNA	0.36	0.03-2.53	
	3-methyl-1,2,3-				
	butanetricarboxylic acid	3-MBTCA	1.07	0.04-7.86	
	3-acetylglutaric acid	3-AGA	3.80	0.10-20.6	bCaryT
	3-hydroxy-4,4-dimethylglutaric	3-HDGA	2.33	0.07-12.8	
	β-caryophyllinic acid	b-CA	1.20	0.03-6.18	
	2,3-dihydroxy-4-oxopentanoic acid	DHOPA	3.03	0.06-16.7	
	Phthalic acid	Pht	13.7	1.81-147	Pht
Aromatic polycarboxylic acids	Isophthalic acid	iPh	0.98	0.10-4.05	
	Terephthalic acid	tPh	15.2	0.76-99.2	
	1,2,4-benzentricarboxylic acid	124BTCA	6.24	0.12-80.7	BTCAs
	1,3,5-benzentricarboxylic acid	135BTCA	0.29	BD-2.84	
Biomass burning tracers	3-hydroxybenzoic acid	3-HBA	0.62	0.10-2.81	
	4-hydroxybenzoic acid	4-HBA	0.92	0.12-6.07	
	Syringic acid	SyrinAcid	0.17	BD-1.69	
	Vanillic acid	VaniAcid			VanillicAci
			0.48	0.01-3.97	d
	Galactosan	Galactosan	6.50	0.85-26.1	
	Mannosan	Mannosan	6.19	0.39-29.2	Mannosan
Primary sugars	Levoglucosan	Levo	101.1	10.9-309	Levo
	Mannitol	Mannitol	35.0	3.36-332	

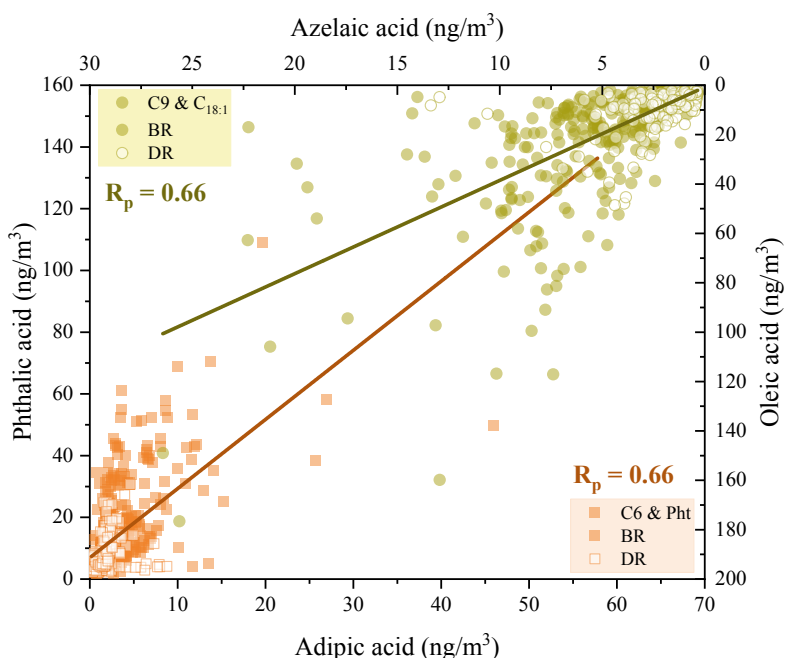
	Glucose	Glucose	4.21	0.58-21.8	
Fatty acids & Cholesterol	Nonanoic acid	C9:0	0.50	0.01-3.33	
	Decanoic acid	C10:0	1.12	BD-7.73	
	Myristic acid	C14:0	0.43	0.07-8.69	
	Pentadecanoic acid	C15:0	0.10	BD-1.57	Saturated
	Palmitic acid	C16:0	6.6	1.05-40.3	fatty acids
	Heptadecanoic acid	C17:0	0.12	BD-2.37	(sFAs)
	Stearic acid	C18:0	8.01	0.79-59.0	
	Nonadecanoic acid	C19:0	0.08	BD-0.58	
	Eicosanoic acid	C20:0	0.24	BD-2.37	
	Oleic acid	C18:1	16.6	0.56-177	Unsaturated
	Palmitoleic acid	C16:1	0.03	0.01-0.44	fatty acids
	Linoleic acid	C18:2	3.36	BD-80.2	(usFAs)
	Cholesterol	Cholesterol	1.22	0.38-5.37	
Alkanes	Heneicosane	n-C21	0.48	0.12-4.60	
	Docosane	n-C22	0.88	0.11-5.86	
	Tricosane	n-C23	1.46	0.27-9.69	
	Tetracosane	n-C24	1.70	0.36-9.16	
	Pentacosane	n-C25	1.75	0.37-10.9	OddAlk
	Hexacosane	n-C26	1.35	0.20-8.78	EvenAlk
	Heptacosane	n-C27	1.31	0.26-9.56	OddAlk
	Octacosane	n-C28	0.76	0.08-7.49	EvenAlk
	Nonacosane	n-C29	1.16	0.03-11.4	OddAlk
	Tracotane	n-C30	0.47	0.01-4.11	EvenAlk
	Hentriacontane	n-C31	0.79	0.01-6.33	OddAlk
	Dotriacontane	n-C32	0.27	0.01-2.63	EvenAlk
	Tritractotane	n-C33	0.34	BD-3.08	
	Tetratriactoane	n-C34	0.20	0.02-1.46	
	Pentatriacontane	n-C35	0.14	BD-1.08	
	Hexatriacontane	n-C36	0.11	BD-0.95	
	Heptatriacontane	n-C37	0.17	BD-15.7	
Hopanes	22,29,30-trisnorhopane	C27Tm	0.02	BD-0.26	
	$\alpha\beta$ -norhopane	C29 $\alpha\beta$	0.06	BD-0.70	
	$\alpha\beta$ -hopane	C30 $\alpha\beta$	0.05	BD-0.52	Hopanes
	$\alpha\beta$ -22S-homohopane	C31 $\alpha\beta$S$$	0.03	BD-0.22	
	$\alpha\beta$ -22R-homohopane	C31 $\alpha\beta$R$$	0.02	BD-0.27	
PAHs	Phenanthrene	Phe	0.14	0.03-0.43	
	Fluoranthene	Flu	0.17	0.01-0.74	
	Pyrene	Pyr	0.15	BD-0.56	
	Benzo[c]phenanthrene	BcP	0.05	BD-0.33	
	Cyclopenta[cd]pyrene	CcdP	0.10	BD-0.55	
	Triphenylene	TriP	0.23	BD-2.08	
	Chrysene	Chr	0.42	BD-3.77	
	Benzo[a]anthracene	BaA	0.13	BD-1.00	

Benzo[b]fluoranthene	BbF	0.18	0.01-1.48	
Benzo[k]fluoranthene	BkF	0.20	0.01-0.92	PAHs252
Benzo[a]fluoranthene	BaF	0.10	BD-0.72	
Benzo[e]pyrene	BeP	0.22	BD-1.54	PAHs252
Benzo[a]pyrene	BaP	0.17	BD-2.02	
Perylene	Per	0.03	BD-0.34	
Indeno[1,2,3-cd]pyrene	IcdP	0.29	BD-2.64	
Benzo[ghi]perylene	BghiP	0.24	BD-1.78	PAHs276

63

64

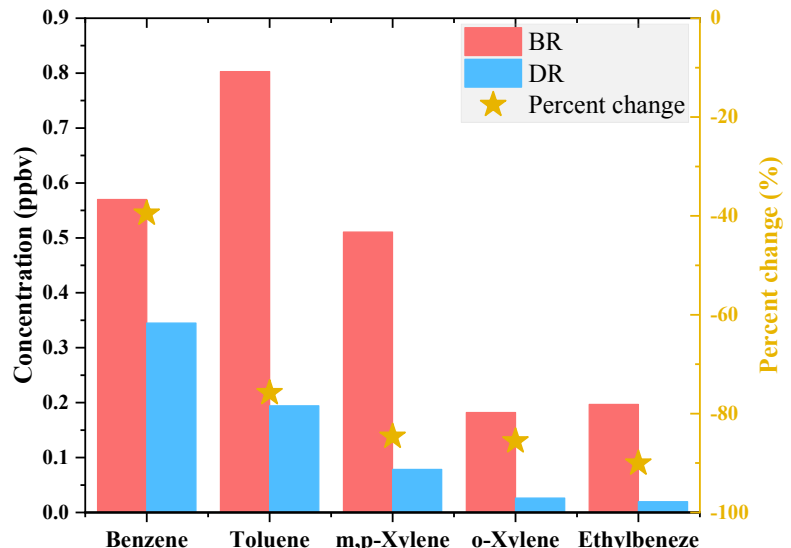
65



66

67 **Figure S4.** Correlation plots of adipic acid (C<sub>6</sub>-DCA) versus phthalic acid (Pht) and azelaic  
 68 acid (C<sub>9</sub>-DCA) versus oleic acid. The data from BR and DR periods are distinguished in  
 69 different colors while the correlation coefficient ( $R_p$ ) values are derived from combined BR  
 70 and DR data.

71



72 **Figure S5.** Stage-wide averaged concentrations of four monoaromatic VOCs and the  
73 percentage changes in their concentrations from BR to DR stage.

74

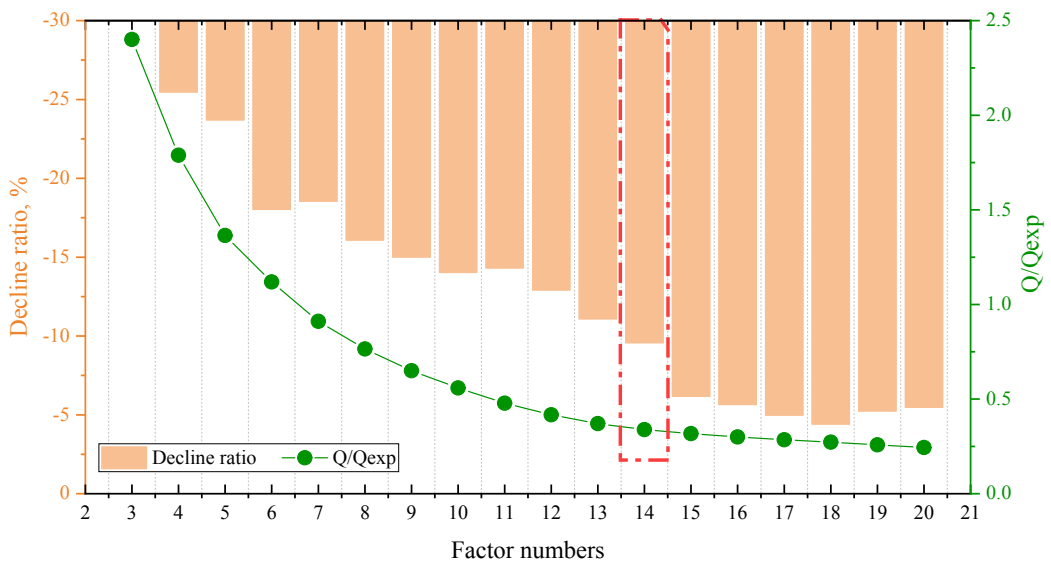
---

75 **Text S2. PMF modeling diagnostics**

76       The input data matrix is a dataset of  $480 \times 27$ , consisting of 480 hourly samples and 27  
77 lumped or individual species in each hourly sample. Three to 20 factors were initially tried in  
78 the PMF model. The  $Q/Q_{\text{exp}}$  ratio, which represents the ratio between the actual sum of the  
79 squares of the scaled residuals ( $Q$ ) (obtained from the PMF least square fit) and the ideal  $Q$   
80 ( $Q_{\text{exp}}$ ) (obtained if the fit residuals at each point were equal to the noise specified for each data  
81 point),<sup>1</sup> was applied to seek the optimal factor numbers. A PMF solution of a certain factor  
82 number with a lower  $Q/Q_{\text{exp}}$  value normally indicates a more robust result.<sup>2</sup> Figure S6 shows a  
83 diagnostic plot of the  $Q/Q_{\text{exp}}$  value versus factor number. The  $Q/Q_{\text{exp}}$  value had a decline trend  
84 with the increase of factor number and ranged from 0.24 to 2.40 (Figure S6). The  $Q/Q_{\text{exp}}$   
85 changed by 6% from the 14- to 15-factor solution, less significant than the 10–25% observed  
86 when the number of factors varied from 3 to 13 (Figure S6), suggesting the factor number  
87 reaching 14 was needed for explaining the input data. The 14-factor solution also provides  
88 explainable source profiles. Thus, it was chosen as the optimal solution.

89       The stability of the 14-factor solution was also assessed by performing two commonly  
90 used error estimation methods provided in the PMF model, namely bootstrap (BS) and  
91 displacement (DISP). The BS method evaluates effect of random errors by recomputing the  
92 model solution with randomly selecting non-overlapping blocks of consecutive samples and  
93 comparing the correlation between the BS run factor and the base run factor.<sup>3</sup> A robust solution  
94 with lower effect from random errors normally demonstrates higher degree of mappings in BS  
95 results. In addition to the BS method, the DISP method estimates effect of rotational ambiguity  
96 by displacing the fitted value of each species in factors far enough to achieve predetermined  
97 increase value for  $Q$  ( $dQ^{\max}$ ). Swaps occur when factors change so much that they exchange  
98 identities, indicating that the solution is not sufficiently robust to be used due to the significant  
99 rotational ambiguity.<sup>4</sup> The BS and DISP results in this study show that all the 14 source factors  
100 resolved in the base run were mapped over 93% of BS runs (Table S2). Neither factor swap or  
101  $Q$  change occurred with DISP estimation. Therefore, the 14-factor solution is quite robust.  
102 Figure S7 shows an excellent correlation between reconstructed  $\text{PM}_{2.5}$  mass concentrations by  
103 summing up all resolved 14 source factors and the measured  $\text{PM}_{2.5}$  mass concentrations, also  
104 confirming that the 14-factor solution appropriately models the measured  $\text{PM}_{2.5}$  concentrations.  
105

106

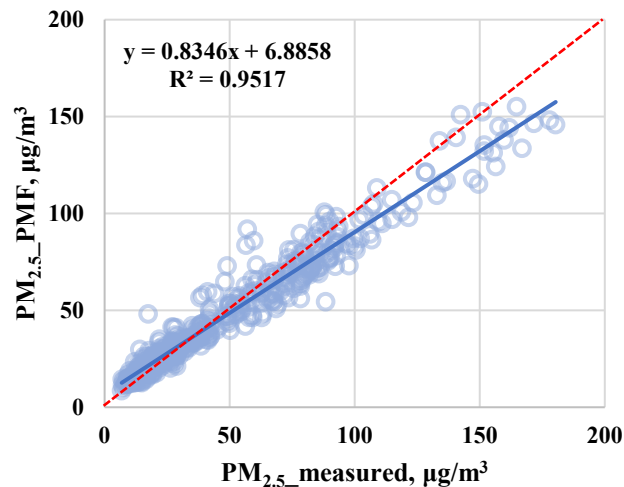


107

108 **Figure S6.** The  $Q/Q_{\text{exp}}$  ratios obtained from PMF solution with a factor number from 3 to 20.  
 109 The 14-factor solution is determined to be the optimal solution and highlighted with red dash  
 110 rectangle in the figure.

111

112

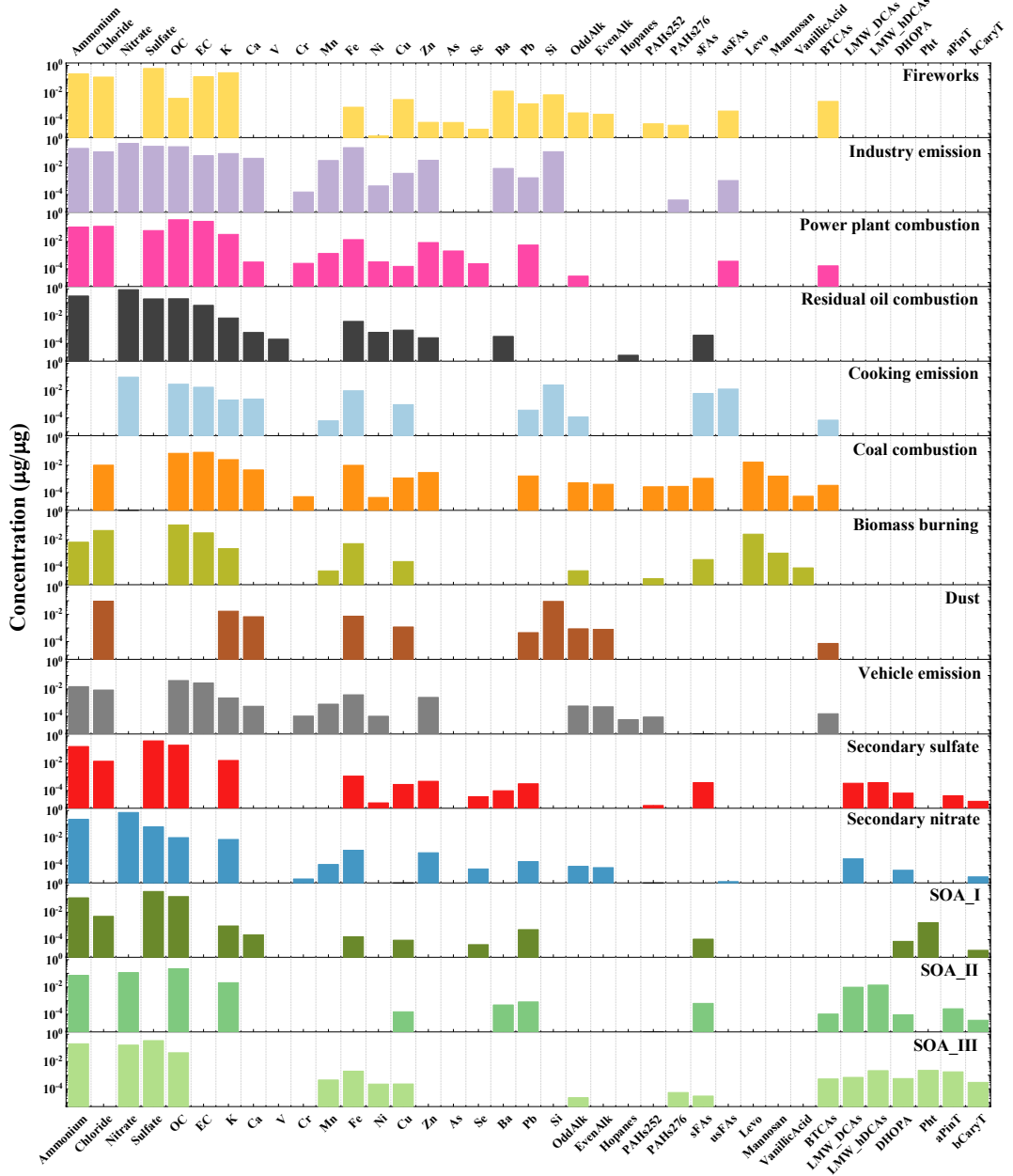


113

114 **Figure S7.** Comparison of reconstructed  $\text{PM}_{2.5}$  mass obtained from the 14-factor PMF solution  
 115 versus measured  $\text{PM}_{2.5}$  mass.

116

117



118

119 **Figure S8.** Source profiles in mass fractions of input species resolved by PMF model.

120

---

121 **Table S2.** Summary of error estimation diagnostics from BS and DISP for PMF model (F1: fireworks, F2: industry emission, F3: power plant combustion, F4:  
122 residual oil combustion, F5: cooking emission, F6: coal combustion, F7: biomass burning, F8: dust, F9: vehicle emission, F10: secondary sulfate, F11: secondary  
123 nitrate, F12: SOA\_I, F13: SOA\_II, F14:SOA\_III).

BS mapping	F1	F2	F3	F4	F5	F6	F7	F8	F9	F10	F11	F12	F13	F14	Unmap ped
F1	100	0	0	0	0	0	0	0	0	0	0	0	0	0	0
F2	0	100	0	0	0	0	0	0	0	0	0	0	0	0	0
F3	0	0	100	0	0	0	0	0	0	0	0	0	0	0	0
F4	0	0	0	100	0	0	0	0	0	0	0	0	0	0	0
F5	0	0	0	0	100	0	0	0	0	0	0	0	0	0	0
F6	0	0	0	0	0	100	0	0	0	0	0	0	0	0	0
F7	0	0	0	0	0	2	97	0	0	0	0	0	0	0	1
F8	0	3	0	0	0	2	0	93	1	0	0	0	0	0	1
F9	0	0	0	0	0	0	0	0	100	0	0	0	0	0	0
F10	0	0	0	0	0	0	0	0	0	100	0	0	0	0	0
F11	0	0	0	0	0	0	0	0	0	0	100	0	0	0	0
F12	0	0	0	0	0	0	0	0	0	0	1	97	0	0	2
F13	0	0	0	0	0	0	0	0	0	0	0	0	100	0	0
F14	0	0	0	0	0	0	0	0	0	0	1	0	0	98	1
DISP diagnostics	Error code: 0							Largest decrease in Q: 0							
Swaps by factor	0	0	0	0	0	0	0	0	0	0	0	0	0	0	0

125 **Table S3.** Correlation (Pearson R) coefficients among PMF-resolved factors and regular pollutants, meteorological parameters (F1: fireworks, F2: industry  
 126 emission, F3: power plant combustion, F4: residual oil combustion, F5: cooking emission, F6: coal combustion, F7: biomass burning, F8: dust, F9: vehicle  
 127 emission, F10: secondary sulfate, F11: secondary nitrate, F12: SOA\_I, F13: SOA\_II, F14:SOA\_III).

Factors*	F1	F2	F3	F4	F5	F6	F7	F8	F9	F10	F11	F12	F13	F14
<b>CO</b>	0.336	0.211	<b>0.672</b>	-0.418	0.147	0.461	0.495	0.401	0.418	0.403	0.778	0.513	0.137	0.370
<b>NO</b>	-0.055	<b>0.579</b>	0.195	0.005	0.264	0.621	0.049	0.070	<b>0.648</b>	-0.144	0.044	-0.041	-0.058	0.144
<b>NO<sub>2</sub></b>	-0.182	<b>0.506</b>	<b>0.355</b>	0.067	0.488	0.432	0.222	0.255	0.466	-0.242	0.449	0.298	-0.014	0.472
<b>SO<sub>2</sub></b>	0.203	0.356	<b>0.509</b>	-0.207	0.052	0.371	0.243	0.393	0.384	0.191	0.610	0.284	-0.038	0.317
<b>O<sub>3</sub></b>	0.124	-0.401	-0.157	-0.079	-0.345	-0.484	-0.102	-0.044	-0.476	0.268	-0.141	-0.010	0.162	-0.263
<b>Ox</b>	-0.058	0.056	0.211	-0.023	0.112	-0.142	0.127	0.251	-0.092	0.073	0.342	0.347	0.211	0.208
<b>Temperature</b>	-0.226	0.249	-0.040	0.154	0.060	-0.055	-0.068	-0.037	-0.005	-0.238	-0.236	-0.122	0.092	0.087
<b>RH</b>	-0.165	0.039	-0.048	0.286	0.037	0.090	0.041	-0.098	0.114	-0.219	-0.162	-0.189	0.064	0.119
<b>Pressure</b>	-0.087	-0.102	-0.165	0.015	-0.026	-0.112	-0.224	0.023	-0.045	0.130	-0.016	-0.047	0.018	-0.068
<b>Visibility</b>	-0.249	-0.189	-0.555	0.144	-0.056	-0.419	-0.482	-0.230	-0.427	-0.295	-0.625	-0.376	-0.274	-0.437
<b>WS</b>	0.027	-0.104	-0.027	-0.052	-0.209	-0.151	-0.093	-0.025	-0.182	0.014	-0.227	-0.051	-0.179	-0.150
<b>PBL</b>	0.251	-0.128	-0.071	-0.075	-0.224	0.041	-0.033	-0.008	0.029	0.148	0.093	-0.018	-0.042	-0.017
<b>Geological materials</b>	-0.083	0.908	0.492	-0.062	0.187	0.428	0.162	<b>0.505</b>	0.585	-0.070	0.322	0.196	-0.079	0.389
<b>POA</b>	0.292	0.298	<b>0.831</b>	-0.291	0.101	<b>0.472</b>	<b>0.539</b>	<b>0.411</b>	<b>0.533</b>	0.356	0.884	0.563	0.102	0.367
<b>SOA</b>	0.506	-0.113	0.506	-0.516	-0.065	0.140	0.402	0.397	0.094	<b>0.644</b>	<b>0.620</b>	<b>0.446</b>	0.216	0.179
<b>Toluene</b>	-0.064	0.508	0.511	-0.090	0.280	0.500	0.188	0.232	<b>0.521</b>	-0.045	0.346	0.217	-0.036	0.364
<b>HOA**</b>	0.309	0.558	0.307	-0.089	0.361	0.639	0.274	0.107	<b>0.685</b>	-0.043	0.154	-0.028	0.188	0.165
<b>COA**</b>	0.359	0.182	0.245	-0.154	<b>0.628</b>	0.239	0.333	0.226	0.118	-0.027	0.236	0.163	0.265	0.078
<b>LVOOA**</b>	0.292	0.247	0.356	-0.404	0.048	0.380	0.467	0.333	0.367	<b>0.578</b>	<b>0.921</b>	<b>0.545</b>	<b>0.456</b>	<b>0.606</b>

128 \*SVOOA obtained from AMS was not included in the table since it did not show strong correlations with PMF-resolved source factors.

129 \*\*Comparisons among AMS-resolved OA factors and PMF-resolved source factors are limited to data for BR stage, as AMS data was not available for the DR period.

130 **Table S4.** Mass contributions of 14-resolved PMF factors to  $\text{PM}_{2.5}$  under each cluster at both BR and DR stages in units of  $\mu\text{g}/\text{m}^3$  (F1: fireworks, F2: industry  
 131 emission, F3: power plant combustion, F4: residual oil combustion, F5: cooking emission, F6: coal combustion, F7: biomass burning, F8: dust, F9: vehicle  
 132 emission, F10: secondary sulfate, F11: secondary nitrate, F12: SOA\_I, F13: SOA\_II, F14:SOA\_III).

Factors	CL#1		CL#2		CL#3		CL#4		Total	
	BR	DR	BR	DR	BR	DR	BR	DR	BR	DR
<b>F1</b>	0.26	0.46	0.49	3.61	0.54	0.77	1.12	6.04	0.51	1.93
<b>F2</b>	0.69	0.14	0.96	0.30	1.27	0.28	0.48	0.27	0.87	0.21
<b>F3</b>	0.87	0.77	2.68	1.20	1.29	0.28	3.00	1.59	1.75	0.92
<b>F4</b>	1.67	0.86	0.43	0.26	1.32	1.48	0.25	0.05	1.06	0.67
<b>F5</b>	1.09	0.64	1.02	0.72	2.18	0.70	2.62	0.75	1.56	0.68
<b>F6</b>	1.01	0.37	2.56	0.81	1.75	0.40	3.49	0.47	1.95	0.51
<b>F7</b>	2.25	2.05	2.99	3.84	3.37	1.57	4.58	4.98	3.05	2.80
<b>F8</b>	1.62	1.80	3.05	2.32	2.18	1.00	4.92	1.51	2.61	1.84
<b>F9</b>	2.81	0.47	6.53	1.01	4.97	0.15	4.79	0.68	4.59	0.61
<b>F10</b>	4.05	7.62	9.10	18.6	4.07	4.99	5.18	21.4	5.54	11.8
<b>F11</b>	12.4	3.21	36.2	17.7	11.0	14.4	38.1	21.7	22.0	10.2
<b>F12</b>	4.87	2.88	10.4	2.84	4.29	2.22	17.6	7.21	8.00	3.23
<b>F13</b>	1.65	2.71	1.39	2.22	2.15	6.15	2.45	3.28	1.82	2.96
<b>F14</b>	2.40	0.71	3.04	0.91	2.20	0.57	1.49	0.58	2.39	0.74
<b>Combined Primary factors</b>	12.3	7.56	20.7	14.1	18.9	6.63	25.3	16.3	18.0	10.2
<b>Combined Secondary factors</b>	25.3	17.1	60.0	42.3	23.8	28.4	64.8	54.2	39.7	29.0

133

134 **Table S5.** Mass contributions of 14-resolved PMF factors to OC under each cluster at both BR and DR stages in units of  $\mu\text{gC}/\text{m}^3$  (F1: fireworks, F2: industry  
 135 emission, F3: power plant combustion, F4: residual oil combustion, F5: cooking emission, F6: coal combustion, F7: biomass burning, F8: dust, F9: vehicle  
 136 emission, F10: secondary sulfate, F11: secondary nitrate, F12: SOA\_I, F13: SOA\_II, F14:SOA\_III).

Factors	CL#1		CL#2		CL#3		CL#4		Total	
	BR	DR	BR	DR	BR	DR	BR	DR	BR	DR
<b>F1</b>	0.00	0.00	0.00	0.01	0.00	0.00	0.00	0.02	0.00	0.01
<b>F2</b>	0.22	0.04	0.31	0.10	0.41	0.09	0.15	0.09	0.28	0.07
<b>F3</b>	0.34	0.30	1.06	0.47	0.51	0.11	1.19	0.63	0.69	0.37
<b>F4</b>	0.32	0.16	0.08	0.05	0.25	0.28	0.05	0.01	0.20	0.13
<b>F5</b>	0.03	0.02	0.03	0.02	0.07	0.02	0.08	0.02	0.05	0.02
<b>F6</b>	0.29	0.11	0.73	0.23	0.50	0.11	0.99	0.13	0.55	0.14
<b>F7</b>	0.27	0.25	0.37	0.47	0.41	0.19	0.56	0.61	0.37	0.34
<b>F8</b>	0.00	0.00	0.00	0.00	0.00	0.00	0.00	0.00	0.00	0.00
<b>F9</b>	0.45	0.08	1.05	0.16	0.80	0.02	0.77	0.11	0.74	0.10
<b>F10</b>	0.86	1.61	1.92	3.93	0.86	1.05	1.09	4.53	1.17	2.50
<b>F11</b>	0.13	0.03	0.38	0.19	0.12	0.15	0.40	0.23	0.23	0.11
<b>F12</b>	0.70	0.41	1.48	0.41	0.61	0.32	2.52	1.03	1.14	0.46
<b>F13</b>	0.36	0.59	0.30	0.49	0.47	1.35	0.54	0.72	0.40	0.65
<b>F14</b>	0.11	0.03	0.14	0.04	0.10	0.03	0.07	0.03	0.11	0.03
<b>Combined Primary factors</b>	1.92	0.96	3.63	1.51	2.95	0.82	3.79	1.62	2.88	1.18
<b>Combined Secondary factors</b>	2.16	2.67	4.22	5.06	2.16	2.90	4.62	6.54	3.05	3.75

---

## 138 References

- 139 1 L. He, X. Huang, L. Xue, M. Hu, Y. Lin, J. Zheng, R. Zhang and Y. Zhang, *Journal of*  
140      *Geophysical Research: Atmospheres*, 2011, **116**, n/a (DOI:10.1029/2010JD014566).
- 141 2 I. M. Ulbrich, M. R. Canagaratna, Q. Zhang, D. R. Worsnop and J. L. Jimenez, *Atmospheric*  
142      *Chemistry and Physics*, 2009, **9**, 2891-2918 (DOI:10.5194/acp-9-2891-2009).
- 143 3 S. G. Brown, S. Eberly, P. Paatero and G. A. Norris, *Sci. Total Environ.*, 2015, **518-519**,  
144      626-635 (DOI:10.1016/j.scitotenv.2015.01.022).
- 145 4 Paatero, P., & Tapper, U. Positive matrix factorization—A nonnegative factor model with  
146      optimal utilization of error-estimates of data values. *Environmetrics*, 1994, **5**, 111–126 (DOI:  
147      10.1002/env.3170050203).
- 148